Proceedings of Symposia in Applied Mathematics

# Reduced Basis Method for Explicit Finite Volume Approximations of Nonlinear Conservation Laws

Bernard Haasdonk and Mario Ohlberger

Abstract. The numerical solution of parametrized partial differential equations ($P^2$DEs ) can be a very time-consuming task if many parameter constellations have to be simulated by high-resolution schemes. Such scenarios may occur in parameter studies, optimization, control, inverse problems or statistical analysis of a given $P^2$DE . Reduced Basis (RB) methods allow to produce fast reduced models that are good surrogates for the detailed numerical scheme and allow parameter variations. These methods have gained increasing attention in recent years for stationary elliptic and instationary parabolic problems.

In the current presentation we present a RB method which is applicable to nonlinear conservation laws with explicit finite volume discretizations. We show that the resulting RB-method is able to capture the evolution of both smooth and discontinuous solutions. In case of symmetries of the problem, the approach realizes an automatic and intuitive space-compression or even space-dimensionality reduction. We perform empirical investigations of the error convergence and runtimes. In all cases we obtain a runtime acceleration of at least one order of magnitude.

## 1. Introduction

We address the task of model reduction for *parametrized* evolution equations. These are problems which are characterized by a parameter vector $\boldsymbol{\mu} \in \mathcal{P}$ from some set of possible parameters $\mathcal{P} \subset \mathbb{R}^p$. The evolution problem then consists of determining $u(x,t;\boldsymbol{\mu})$ on a bounded domain $\Omega \subset \mathbb{R}^d$ and finite time interval $[0,T], T > 0$ such that

$$\partial_t u(\boldsymbol{\mu}) + \mathcal{L}(t;\boldsymbol{\mu})(u(t;\boldsymbol{\mu})) = 0, \quad u(0;\boldsymbol{\mu}) = u_0(\boldsymbol{\mu}), \tag{1.1}$$

and suitable boundary conditions are satisfied. Here $u_0(\boldsymbol{\mu})$ are the parameter-dependent initial values, $\mathcal{L}(t;\boldsymbol{\mu})$ is the parameter dependent spatial differential operator. Usually, the initial values and solution have some spatial regularity $u_0(\boldsymbol{\mu}), u(t;\boldsymbol{\mu}) \in \mathcal{W} \subset L^2(\Omega)$.

---

1991 *Mathematics Subject Classification.* Primary 76M12, 35L90; Secondary 76R99.

*Key words and phrases.* Model Reduction, Reduced Basis Methods, Parameter Dependent Explicit Operators, Empirical Interpolation .

The authors were supported by the Landesstiftung Baden Württemberg gGmbH and the German Federal Ministry of Education and Research under grant number 03SF0310C.

©0000 (copyright holder)

Evolution schemes produce discrete solutions $u_H^k(\boldsymbol{\mu}) \in \mathcal{W}_H, k = 0, \ldots, K$ in an $H$-dimensional discrete space $\mathcal{W}_H \subset L^2(\Omega)$ approximating $u(t^k; \boldsymbol{\mu})$ at the time instants $0 = t^0 < t^1 < \ldots < t^K = T$. Such detailed simulations are frequently expensive to compute due to the high space resolution and not suitable for use in multi-query settings, i.e. multiple simulation requests with varying parameters $\boldsymbol{\mu}$.

Reduced Basis (RB) methods are increasingly popular methods to solve such parametrized problems, aiming at reduced simulation schemes, which approximate the detailed solutions $u_H^k(\boldsymbol{\mu})$ by efficiently computed reduced solutions $u_N^k \in \mathcal{W}_N$. Here $\mathcal{W}_N \subset L^2(\Omega)$ is an $N$-dimensional reduced basis space with suitable reduced basis $\Phi_N$. The latter is generated in a problem specific way based on snapshots of discrete solutions. Reduced basis methods in particular have been applied successfully for various elliptic and parabolic problems, almost exclusively based on finite element discretizations. For linear elliptic problems we refer to [**PR07**], linear parabolic equations are treated in [**GP05**], extensions to nonlinear equations [**VPP03, Gre05**] or systems [**Roz05**] have been developed. We have proposed an RB-formulation for linear finite volume (FV) schemes [**HO08b**] in case of so called *affine parameter dependence* of the data functions. We recently have extended this RB-scheme to explicit discretizations with general parameter dependence and demonstrated the applicability to a linear evolution problem [**HOR07**].

In the current presentation, we adopt the latter methodology to nonlinear conservation laws with explicit finite volume schemes. The structure of our paper is as follows. Section 2 explains the RB approach for general explicit discretization schemes. The key ingredient in the scheme is an *empirical interpolation* step for approximating the non-linear discrete spatial differential operator evaluations. Then a Galerkin projection step based on the reduced basis space defines the overall RB-scheme. In the experimental Section 3 we demonstrate the applicability of the method on both smooth and discontinuous data subject to nonlinear convection. Experimentally, we investigate the approximation properties and demonstrate the runtime gain compared to the full FV schemes. We conclude in Section 4.

## 2. Reduced Basis Method for Nonlinear Finite Volume Schemes

We now specify the considered nonlinear FV discretizations and present the corresponding RB simulation scheme.

**2.1. Nonlinear Finite Volume Schemes.** As special instances of the general evolution equation (1.1) we consider the following scalar nonlinear conservation law on a polygonal domain $\Omega \subset \mathbb{R}^2$:

$$\partial_t u(t;\boldsymbol{\mu}) + \nabla \cdot f(u(t;\boldsymbol{\mu});\boldsymbol{\mu}) = 0 \quad \text{in} \quad \Omega \times [0,T] \tag{2.1}$$

with suitable parametrized flux function $f(\cdot;\boldsymbol{\mu})$, initial data $u(0;\boldsymbol{\mu}) = u_0(\boldsymbol{\mu})$ in $\Omega$, Dirichlet boundary data $u(\boldsymbol{\mu}) = u_{\text{dir}}(\boldsymbol{\mu})$ on $\Gamma_{\text{dir}} \times [0,T]$, Neumann boundary values $f(u(\boldsymbol{\mu});\boldsymbol{\mu}) \cdot \mathbf{n} = u_{\text{neu}}(\boldsymbol{\mu})$ on $\Gamma_{\text{neu}} \times [0,T]$ and possibly (for special geometries) periodic boundary conditions on the remaining boundary $\partial\Omega \backslash (\Gamma_{\text{dir}} \cup \Gamma_{\text{neu}})$.

We denote $\mathcal{W} := L^\infty(\Omega) \cap BV(\Omega) \subset L^2(\Omega)$ as the exact solution space with respect to the space variable. As numerical scheme we use an explicit first order FV scheme. We assume a numerical grid $\mathcal{T} := \{e_i\}_{i=1}^H$ of $H$ disjoint convex polygonal elements, which form a partition of the domain $\bar{\Omega} = \bigcup_{i=1}^H \bar{e}_i$. This specifies the space of elementwise constant functions $\mathcal{W}_H$, which is obviously $H$ dimensional

with usually large $H$. In the following, $\mathcal{W}_H$ will be denoted more generally as detailed discretization space.

For simplicity we define $t^k := k\Delta t$ with a global time-step size $\Delta t > 0$, which is small enough such that it satisfies a CFL condition and we reach the end time $t^K = T$. For an element $e_i$ we use $\mathcal{N}(i)$ as an index set for its edges. The $j$-th edge of $e_i$ will be denoted as $e_{ij}$ with outer normal $\mathbf{n}_{ij}$. Then, a FV scheme produces a sequence of solutions $\{u_H^k\}_{k=0}^K \subset \mathcal{W}_H$ by evolution in time via

$$u_i^0 := \frac{1}{|e_i|}\int_{e_i} u_0, \quad u_i^{k+1} := u_i^k - \frac{\Delta t}{|e_i|}\sum_{j\in\mathcal{N}(i)} g_{ij}^k(u_i^k, u_{ij}^k). \tag{2.2}$$

Here $u_i^k$ denotes the cell value of $u_H^k$ on element $e_i$, $|e_i|$ denotes the area of the element and $g_{ij}^k(u,v)$ denotes a numerical flux. For inner (and periodic) edges, $u_{ij}^k$ is the value of $u_H^k$ across the edge $j$. For Dirichlet boundary edges, $u_{ij}^k$ is the Dirichlet value averaged on the edge $u_{ij} := \frac{1}{e_{ij}}\int_{e_i} u_{\mathrm{dir}}$. For Neumann edges $e_{ij}$ the value $u_{ij}^k$ can be chosen arbitrarily as $g_{ij}$ then is not depending on its arguments, instead the numerical flux is specified by the Neumann boundary function $g_{ij}^k(u_i^k, u_{ij}^k) := \int_{e_{ij}} u_{\mathrm{neu}}$. For inner, periodic and Dirichlet boundary edges $e_{ij}$, we use the Engquist-Osher flux in order to obtain low numerical viscosity in the schemes. This can be expressed by setting $c_{ij}(u) := \mathbf{n}_{ij} f(u)$ for all edges, defining

$$c_{ij}^+(u) := c_{ij}(0) + \int_0^u \max(c_{ij}'(s), 0)ds, \quad c_{ij}^-(u) := \int_0^u \min(c_{ij}'(s), 0)ds$$

and then choosing the numerical flux $g_{ij}^k(u,v) := |e_{ij}|[c_{ij}^+(u) + c_{ij}^-(v)]$, cf. [**Krö97**]. We can rewrite this FV scheme in a more simple form if we denote the cell averaging of the initial data as a general projection operator $P : \mathcal{W} \to \mathcal{W}_H$ and the space discretization operator as $\mathcal{L}_E(t;\boldsymbol{\mu}) : \mathcal{W}_H \to \mathcal{W}_H$. Then, the explicit FV scheme is compactly expressed as

$$u_H^0 := P[u_0], \quad u_H^{k+1} := u_H^k - \Delta t \mathcal{L}_E(t;\boldsymbol{\mu})[u_H^k], \quad k = 0, \dots, K-1. \tag{2.3}$$

Note, that the following interpolation procedure and the reduced basis scheme will be based on these generalized notions and is thus also applicable to other evolution problems, discrete function spaces and discretization operators, e.g. finite element or discontinuous Galerkin methods.

**2.2. Empirical Interpolation.** The application of the general evolution operator $\mathcal{L}_E(t;\boldsymbol{\mu})[v_H]$ on a function $v_H \in \mathcal{W}_H$ is obviously both space and parameter dependent. Hence the complexity of the computation for each new parameter is depending on $H$. This can be accelerated for typical discretization operators by suitable approximations of the form

$$\mathcal{I}_M[\mathcal{L}_E(t;\boldsymbol{\mu})[v_H]] := \sum_{m=1}^M \xi_m l_m(t;\boldsymbol{\mu})[v_H] \approx \mathcal{L}_E(t;\boldsymbol{\mu})[v_H] \tag{2.4}$$

with parameter independent but space dependent *collateral reduced basis* $\boldsymbol{\xi}_M := \{\xi_m\}_{m=1}^M \subset \mathcal{W}_H$ and functionals $l_m(t;\boldsymbol{\mu}) : \mathcal{W}_H \to \mathbb{R}$, which must be computable with complexity independent of $H$. One instantiation of such an approximation is the empirical interpolation [**BMNP04**]. This method can briefly be expressed based on a set of interpolation points $T_M := \{x_m\}_{m=1}^M \subset \Omega$ and a corresponding nodal interpolation basis $\boldsymbol{\xi}_M$, i.e. $\xi_m(x_{m'}) = \delta_{m,m'}$ for $1 \le m, m' \le M$. The set

$T_M$ and $\boldsymbol{\xi}_M$ are determined in an extensive offline search procedure: A large set of snapshots $L_{train} := \{\mathcal{L}_E(t^{k_i};\boldsymbol{\mu}_i)[u_H^{k_i}(\boldsymbol{\mu}_i)]\}_{i=1}^{N_{train}}$ is precomputed for a training set of time-instants $t^{k_i}$ and parameters $\boldsymbol{\mu}_i$. Then the collateral basis $\boldsymbol{\xi}_M$ and corresponding interpolation points $T_M$ are determined based on an iterative basis extension process. In every of $M$ iterations, the worst approximated snapshot in $L_{train}$ is determined in a greedy search and a new basis vector and interpolation point are determined from this. In the experiments we applied the collateral reduced basis generation procedure presented in [**HOR07**], which is based on the original method [**BMNP04**]. Due to space constraints, we must refrain from giving more details on this aspect.

For (2.4) being an interpolation, the parameter dependent functionals $l_m(t;\boldsymbol{\mu})$ must simply correspond to point evaluations $l_m(t;\boldsymbol{\mu})[v_H] := \mathcal{L}_E(t;\boldsymbol{\mu})[v_H](x_m)$. This is an operation that can be computed fast if $\mathcal{L}_E(t;\boldsymbol{\mu})$ is a localized discretization operator, i.e. point values of $\mathcal{L}_E(t;\boldsymbol{\mu})[v_H]$ only depend on few neighbouring point values of $v_H$. For instance, finite element and finite volume operators are localized in this sense as a point value of the result only requires the values of $v_H$ on the neighouring grid cells and geometric information of a local subgrid.

**2.3. Reduced Basis Method.** The key ingredient for a good RB scheme is the availability of a suitable low dimensional reduced basis space $\mathcal{W}_N$. In the experiments we apply the reduced basis construction method as presented in [**HO08b**], a more sophisticated method using adaptive grids was given in [**HO08a**]. Detailed presentations of methods for reduced basis generation can be found in [**PR07**]. These methods are inherently accumulative and snapshot-based, as the collateral reduced basis generation schemes mentioned above. Hence, an initially small (or empty) basis is iteratively enriched using solutions $u_H^{k_i}(\boldsymbol{\mu}_i)$ for certain time steps $k_i$ and parameters $\boldsymbol{\mu}_i$. We also refrain from further details here but simply assume the availability of a well-approximating reduced basis $\Phi_N := \{\varphi_n\}_{n=1}^N$ with basis functions $\varphi_n$ and the resulting reduced basis space $\mathcal{W}_N := \operatorname{span}(\Phi_N)$.

The idea for the RB-scheme now is simply replacing the discrete space evolution operator $\mathcal{L}_E(t;\boldsymbol{\mu})[\cdot]$ in (2.3) by the interpolated operator $\mathcal{I}_M[\mathcal{L}_E(t;\boldsymbol{\mu})[\cdot]]$, expressing the equation in a weak form by trial functions $\varphi \in \mathcal{W}_N$ and using $\mathcal{W}_N$ as the ansatz space for the reduced solution $u_N^k$. Hence, we search $u_N^k \in \mathcal{W}_N$ such that for all $k = 0,\dots,K-1$ and $\varphi \in \mathcal{W}_N$ holds

$$(u_N^0,\varphi) = (P[u_0],\varphi), \quad (u_N^{k+1},\varphi) = (u_N^k,\varphi) - \Delta t(\mathcal{I}_M[\mathcal{L}_E(t;\boldsymbol{\mu})[u_N^k]],\varphi). \tag{2.5}$$

Here we use $(u,v) := \int_\Omega uv$ as an abbreviation of the $L^2$ inner product. We obtain the following reduced basis scheme for determining the unknown basis coefficients of $u_N^k(\boldsymbol{\mu})$.

Definition 2.1 (Reduced Basis Approximation with Empirical Interpolation of $\mathcal{L}_E$). We assume that $\mathcal{L}_E(t^k;\boldsymbol{\mu})$ is an arbitrary explicit space discretization operator. We assume that an appropriate empirical interpolation scheme is defined by means of interpolation basis $\boldsymbol{\xi}_M$ and interpolation points $T_M \subset \Omega$, and a reduced basis $\Phi_N$ is available. We then define the following scheme for sequentially computing $u_N^k(\boldsymbol{\mu}) := \sum_n a_n^k(\boldsymbol{\mu})\varphi_n$ by specifying its coefficient vectors $\mathbf{a}^k = (a_1^k,\dots,a_N^k)^T \in \mathbb{R}^N$ for $k = 0,\dots,K$:

$$\mathbf{a}^0 := \left((P[u_0(\boldsymbol{\mu})],\varphi_1),\dots,(P[u_0(\boldsymbol{\mu})],\varphi_N)\right)^T, \tag{2.6}$$

$$\mathbf{a}^{k+1} = \mathbf{a}^k - \Delta t\mathbf{C}_E\mathbf{l}_E(\boldsymbol{\mu},t^k)[\mathbf{a}^k]. \tag{2.7}$$

Here, the corresponding vectors and matrices are defined as

$$(\mathbf{C}_E)_{nm} := (\xi_m, \varphi_n)\,, \tag{2.8}$$

$$\left(\mathbf{l}_E(\boldsymbol{\mu}, t^k)[\mathbf{a}^k]\right)_m := \mathcal{I}_M[\mathcal{L}_E(t^k; \boldsymbol{\mu})[u_N^k]](x_m) \tag{2.9}$$

for $n = 1, \ldots, N$ and $m = 1, \ldots, M$. The resulting sequence of functions $\{u_N^k(\boldsymbol{\mu})\}_{k=0}^K$ finally defines the *reduced basis approximation* $u_N(t; \boldsymbol{\mu})$ that coincides with $u_N^k(\boldsymbol{\mu})$ in the time-slab $[t^k, t^{k+1})$.

This scheme allows a full offline/online decomposition in case of a localized discretization operator and initial data of the form $u_0(x, \boldsymbol{\mu}) = \sum_{q=1}^Q \sigma^q(\boldsymbol{\mu}) u_0^q(x)$. In the offline phase, the quantities $\Phi, \boldsymbol{\xi}_M, C_E, T_M$, a numerical subgrid and the components $\mathbf{a}^{0,q}$ (analogous to (2.6) but using $u_0^q$) are determined. In the online phase these quantities are used for fast reduced simulation by starting with $\mathbf{a}^0 = \sum_{q=1}^Q \sigma^q(\boldsymbol{\mu}) \mathbf{a}^{0,q}$ and proceeding by (2.7). This is the key for efficient and fast online simulation. In essence, the complexity of a reduced simulation step is not depending on the detailed space dimensionality $H$ but only polynomial in the reduced dimensionalities $N$ and $M$. Further, rigorous a-posteriori error estimators can be derived which can also be computed rapidly in an offline/online fashion. For details on these aspects we refer to [**HOR07**].

## 3. Experiments

For simplicity we use a discretization on uniform Cartesian grids. The specific flux functions, initial data, boundary conditions, and parametrization are specified in each of the following examples The implementation is based on our MATLAB package *RBmatlab*.

**3.1. Nonlinear Convection.** In a first example, we want to demonstrate the applicability for increasingly nonlinear convection with smooth initial data and a single parameter. For this we model a transition between linear transport and the Burgers equation.

We choose $\Omega = [0, 2] \times [0, 1]$ with purely periodic boundary conditions and fix the end time $T = 0.3$. We consider the single parameter $\boldsymbol{\mu} := (p) \in \mathcal{P} := [1, 2]$ for the exponent in the nonlinear flux function $f(u; \boldsymbol{\mu}) := \mathbf{v} u^p$ with the space- and time-constant velocity field $\mathbf{v} = (1, 1)^T$. The initial data is a smooth function $u_0(x) = \frac{1}{2}(1 + \sin(2\pi x_1)\sin(2\pi x_2))$ for $x = (x_1, x_2)^T \in \Omega$. We choose a $120 \times 60$ grid for decomposing $\Omega$. The global CFL condition then holds with $K = 100$ timesteps.

Figure 1 illustrates the initial data (which is independent of $p$) and the final state for $p = 1$ resp. $p = 2$. We nicely see, how the model represents the transition between linear transport ($p = 1$) and the nonlinear non-viscous instationary Burgers equation ($p = 2$), where discontinuities develop during time.

To get an insight into the empirical interpolation procedure, we illustrate the resulting interpolation points $T_M$ for $M = 150$ in Fig. 2. More precisely, we plot the grid cells around the selected points, as the search for possible interpolation points is restricted to the centroids of the grid cells. The order of the point selection is indicated in gray shades. It is visible, how the first – and therefore most important – selected points are lying around the diagonal, i.e. regions corresponding to the extreme values of the solution. A striking point is the localization of the points in the lower left quarter of the domain, which is due to 2 facts: The translation symmetry of the problem defines several equivalent positions for the interpolation

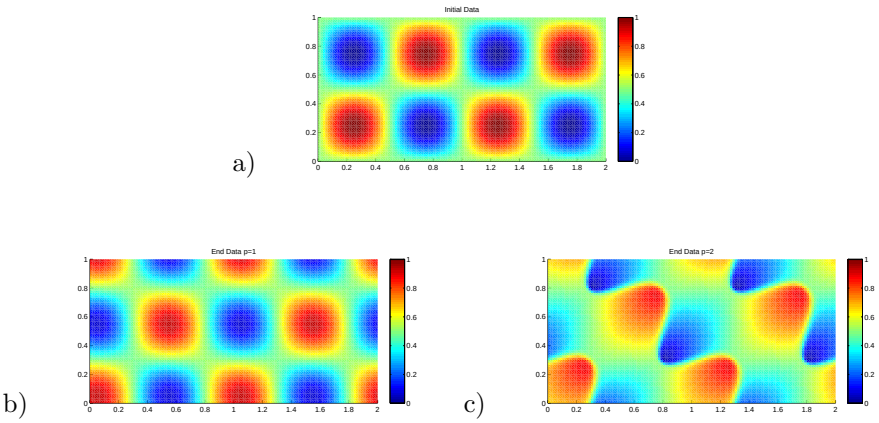


FIGURE 1. Illustration of transport for smooth data. a) Initial data, b) solution at end time for $p = 1$, c) solution at end time for $p = 2$.

points in the different subregions of the domain. The search for the interpolation points now is based on a linear row-wise search from left to right and then bottom to top. Hence, every interpolation point is chosen in the lower left of the domain. This is now an important result from an information-theoretic viewpoint: The model reduction technique can realize space-compression in case of problem symmetries. In Fig. 3 we illustrate the error convergence for the resulting reduced simulation

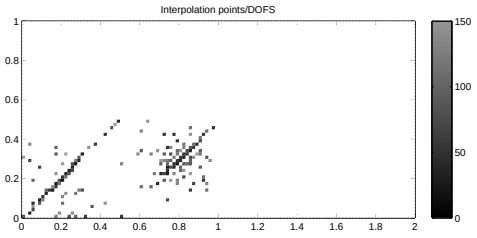


FIGURE 2. Illustration of empirical interpolation point selection for smooth data. The 150 grid cells around the interpolation points are shaded in their selection order.

scheme. We select a set $M_{\text{test}} \subset \mathcal{P}$ of 10 random values for $p$ not used during basis generation and determine $\max_{\boldsymbol{\mu} \in M_{\text{test}}} ||u_N(\boldsymbol{\mu}) - u_H(\boldsymbol{\mu})||_{L^\infty([0,T],L^2(\Omega))}$ for different dimensionalities $N$ and $M$. We plot the resulting maximal error in a logarithmical scale. It can nicely be seen, how a simultaneous increase of $N$ and $M$ reveals almost exponential convergence along the diagonal of the plot. This simultaneous increase is important: If $M$ is fixed, increase of $N$ over a certain limit gives an error increase. If $N$ is fixed, raising $M$ gives no error improvement after a certain limit.

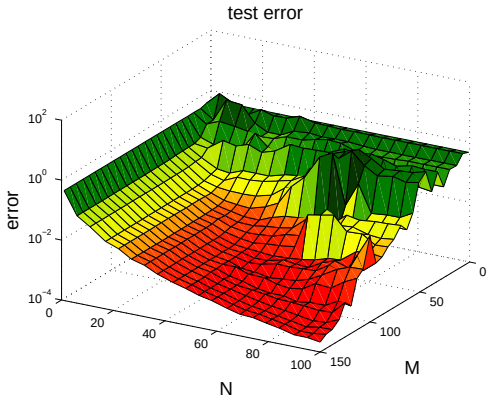


FIGURE 3. Illustration of RB test-error convergence for for continuous initial data with varying dimensionalities $N$ and $M$.

TABLE 1. Runtime comparison for detailed simulation with reduced simulations of varying reduced dimensionalities.

| Simulation | Dimensionality | Runtime [s] |
|---|---|---|
| Detailed | $H = 7200$ | 20.22 |
| Reduced | $N = 20, M = 30$ | 0.91 |
| Reduced | $N = 40, M = 60$ | 1.22 |
| Reduced | $N = 60, M = 90$ | 1.55 |
| Reduced | $N = 80, M = 120$ | 1.77 |
| Reduced | $N = 100, M = 150$ | 2.06 |

The main goal of RB-methods is an accurate approximation under largely reduced simulation time. To assess these computation times, we determine the detailed and reduced simulation times over 10 random parameter drawings and report the average runtimes in Tab. 1. The times were obtained on an IBM Lenovo Notebook (Intel Centrino Duo, 2.0 GHz, 1024 MB RAM). It can nicely be seen, that we obtain acceleration factors of 10-22 depending on the dimensionalities of the reduced simulation.

**3.2. Riemann Problem for Burgers Equation.** In the second example we want to demonstrate the applicability to nonlinear convection by the non-viscous Burgers equation with discontinuous initial data, moving shock and multiple parameters.

We choose $\Omega = [0,1] \times [0,1]$ and fix the end time $T = 0.5$. The Dirichlet boundary consists of the left and right edges of the unit square, while the top and bottom are assigned no-flow Neumann boundary conditions $u_{neu} \equiv 0$. The parametrization consists of the three parameters $\boldsymbol{\mu} = (u_l, u_r, v) \in \mathcal{P} := [-1,1]^3 \subset \mathbb{R}^3$ which model the left and right initial values and the horizontal velocity. Hence, we choose the flux $f(u;\boldsymbol{\mu}) := \mathbf{v}(\boldsymbol{\mu})u^2$ with $\mathbf{v}(\boldsymbol{\mu}) = (v,0)^T$ as space- and time-constant velocity field. The initial data and Dirichlet boundary data is given by a

discontinuous function for $x = (x_1, x_2)^T \in \Omega$ as

$$u_{dir}(x; \boldsymbol{\mu}) = u_0(x; \boldsymbol{\mu}) = \begin{cases} u_l & \text{for } x_1 \leq 0.5, \\ u_r & \text{otherwise.} \end{cases}$$

We choose a $100 \times 100$ grid for decomposing $\Omega$ hence $H = 10000$. The global CFL condition then holds with $K = 100$ timesteps. Figure 4 illustrates the initial data and the final state for the parameters $u_l = 0.0, u_r = 0.5, v = 0.9$ in the upper row, and for $u_l = 0.5, u_r = 1.0, v = -0.5$ in the lower row. We see, how the model represents both rarefaction waves and moving shocks depending on different parameter settings.

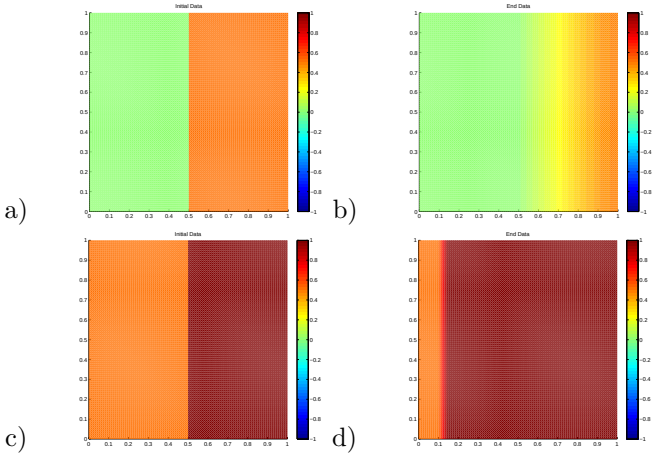


FIGURE 4. Illustration of transport for discontinuous data. a) Initial data and b) solution at end time for $\boldsymbol{\mu} = (0.0, 0.5, 0.9)^T$, c) initial data and d) solution at end time for $\boldsymbol{\mu} = (0.5, 1.0, -0.5)^T$.

We again illustrate the resulting interpolation points $T_M$ by their corresponding grid cells for $M = 100$ in Fig. 5. The interesting fact is the localization of the points. They exactly correspond to the 100 grid cells of a the complete lowest row of the numerical grid. This again is due to the symmetry of the problem (which is inherently a 1D problem extruded to 2D) and the bottom-up search of interpolation point search. We get an even stronger result as before: The model reduction technique can automatically detect the possibility of space-dimension reduction in case of a symmetric problem. Hence, there is no need for a possibly faulty heuristic dimensionality reduction by hand by eliminating some space coordinate directions: The RB method can detect such redundancies based on an automatic procedure.

In Fig. 6 we illustrate the error convergence for the resulting reduced simulation scheme as before based on a set $M_{\text{test}} \subset \mathcal{P}$ of 10 random values and report the maximum $L^\infty(L^2)$ error while varying $N$ and $M$. The difficulty of the problem is expressed by the weakly decaying error. Essentially only for the full resolution $N = M = 100$ we get a sufficiently accurate model. But for these values, the model is perfect.

We again assess the computation times. For the detailed simulation we get the average computation times of 21.20 seconds. As the low dimensional reduced models will not be very accurate, we omit listing their runtimes. We only determine

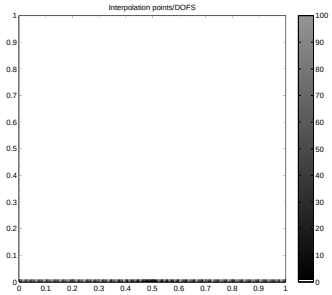


FIGURE 5. Illustration of empirical interpolation point selection for discontinuous data. The 100 grid cells around the interpolation points comprise precisely one row of the grid.

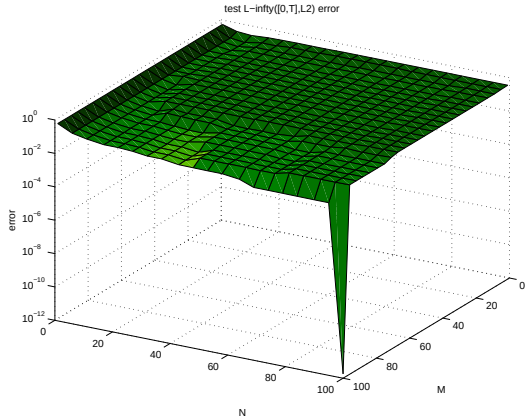


FIGURE 6. Illustration of RB test-error convergence for discontinuous initial data with varying dimensionalities $N$ and $M$

the runtime for the perfect but larger reduced model of order $N = M = 100$. The 10 fold averaged runtime for this model is 1.36 seconds, hence an acceleration factor of 15.6 is realized in this case.

Note that the Cartesian grids and symmetric data functions allowed to demonstrate the space compression abilities of the scheme. Still, the methods also are implemented for unstructured grids. We obtain similar acceleration factors for such grids, but the symmetry and the intuitive interpretation of the interpolation procedure could not be demonstrated so clearly.

## 4. Conclusion

We have presented a reduced basis method for nonlinear explicit evolution schemes exemplified for FV discretizations. RB-methods are not only applicable to elliptic or parabolic problems as mostly done in literature, but also to nonlinear conservation laws. We have shown the suitability for both smooth and discontinuous initial data, with single and multiple parameters. By suitable, fully automatical constructions of the reduced basis and collateral reduced basis, we obtain reduced models, that enable rapid parameter variation with accurate approximations. The

reduced models have shown an acceleration of at least one order of magnitude in all cases. However, the error convergence of the reduced models revealed a difference between smooth and discontinuous data. The error decay was much faster for the smooth data than for the moving shock front. This may offer perspectives for more efficient solution representation: Instead of only linear superpositions of reduced basis vectors, a moving discontinuity might be more efficiently represented by spatial translates or more general spatial transformations of few basis functions. By this we expect lower dimensional models with interesting simulation schemes. We have demonstrated, that the RB methodology resp. the interpolation procedure is able to detect spatial redundancy. In the given examples, it realized not only spatial compression but even symmetry detection and dimensionality reduction. The acceleration for explicit schemes is already considerable as we are able to accelerate the cheap detailed evolution steps of complexity $\mathcal{O}(H)$. In combination with implicit contributions of complexity $\mathcal{O}(H^3)$ we expect much higher acceleration factors.

## References


[BMNP04] M. Barrault, Y. Maday, N.C. Nguyen, and A.T. Patera, *An 'empirical interpolation' method: application to efficient reduced-basis discretization of partial differential equations*, C. R. Math. Acad. Sci. Paris Series I **339** (2004), 667–672.

[GP05] M.A. Grepl and A.T. Patera, *A posteriori error bounds for reduced-basis approximations of parametrized parabolic partial differential equations*, M2AN Math. Model. Numer. Anal. **39** (2005), no. 1, 157–181.

[Gre05] M.A. Grepl, *Reduced-basis approximations and a posteriori error estimation for parabolic partial differential equations*, Ph.D. thesis, Massachusetts Institute of Technology, May 2005.

[HO08a] B. Haasdonk and M. Ohlberger, *Adaptive basis enrichment for the reduced basis method applied to finite volume schemes*, Proc. 5th International Symposium on Finite Volumes for Complex Applications, 2008, pp. 471–478.

[HO08b] ———, *Reduced basis method for finite volume approximations of parametrized linear evolution equations*, M2AN, Math. Model. Numer. Anal. **42** (2008), no. 2, 277–302.

[HOR07] B. Haasdonk, M. Ohlberger, and G. Rozza, *A reduced basis method for evolution schemes with parameter-dependent explicit operators*, Tech. Report 09/07 - N, FB 10, University of Münster, 2007, Accepted by ETNA.

[Krö97] D. Kröner, *Numerical schemes for conservation laws*, John Wiley & Sons and Teubner, 1997.

[PR07] A.T. Patera and G. Rozza, *Reduced basis approximation and a posteriori error estimation for parametrized partial differential equations*, MIT, 2007, Version 1.0, Copyright MIT 2006-2007, to appear in (tentative rubric) MIT Pappalardo Graduate Monographs in Mechanical Engineering.

[Roz05] G. Rozza, *Shape design by optimal flow control and reduced basis techniques: Applications to bypass configurations in haemodynamics*, Ph.D. thesis, École Polytechnique Fédérale de Lausanne, November 2005.

[VPP03] K. Veroy, C. Prud'homme, and A.T. Patera, *Reduced-basis approximation of the viscous Burgers equation: rigorous a posteriori error bounds*, C. R. Math. Acad. Sci. Paris Series I **337** (2003), 619–624.



Institute of Numerical and Applied Mathematics, University of Münster, Einsteinstrasse 62, 48149 Münster, Germany

*E-mail address*: bernard.haasdonk@wwu.de, mario.ohlberger@math.uni-muenster.de